Characterization of enhanced antibacterial effects of novel silver nanoparticles



2007 Nanotechnology 18 225103

(http://iopscience.iop.org/0957-4484/18/22/225103)

IOP PUBLISHING NANOTECHNOLOGY
Nanotechnology **18** (2007) 225103 (9pp) doi:10.1088/0957-4484/18/22/225103

# Characterization of enhanced antibacterial effects of novel silver nanoparticles

**Siddhartha Shrivastava[1,5], Tanmay Bera[2,5], Arnab Roy[1], Gajendra Singh[3], P Ramachandrarao[4] and Debabrata Dash[1,6]**

[1] Department of Biochemistry, Institute of Medical Sciences, Banaras Hindu University, Varanasi-221005, India
[2] Department of Metallurgy, Institute of Technology, Banaras Hindu University, Varanasi-221005, India
[3] Department of Anatomy, Institute of Medical Sciences, Banaras Hindu University, Varanasi-221005, India
[4] Defence Institute of Advanced Technology, Pune-411025, India

E-mail: ddass@satyam.net.in

Received 19 January 2007, in final form 14 February 2007
Published 4 May 2007
Online at stacks.iop.org/Nano/18/225103

**Abstract**
In the present study, we report the preparation of silver nanoparticles in the range of 10–15 nm with increased stability and enhanced anti-bacterial potency. The morphology of the nanoparticles was characterized by transmission electron microscopy. The antibacterial effect of silver nanoparticles used in this study was found to be far more potent than that described in the earlier reports. This effect was dose dependent and was more pronounced against gram-negative bacteria than gram-positive organisms. Although bacterial cell lysis could be one of the reasons for the observed antibacterial property, nanoparticles also modulated the phosphotyrosine profile of putative bacterial peptides, which could thus affect bacterial signal transduction and inhibit the growth of the organisms.

## 1. Introduction

Nanotechnology involves the tailoring of materials at atomic level to attain unique properties, which can be suitably manipulated for the desired applications [1]. Most of the natural processes also take place in the nanometre scale regime. Therefore, a confluence of nanotechnology and biology can address several biomedical problems, and can revolutionize the field of health and medicine [2]. Nanotechnology is currently employed as a tool to explore the darkest avenues of medical sciences in several ways like imaging [3], sensing [4], targeted drug delivery [5] and gene delivery systems [6] and artificial implants [7]. Hence, nanosized organic and inorganic particles are finding increasing attention in medical applications [8] due to their amenability to biological functionalization. Based on enhanced effectiveness, the new age drugs are nanoparticles of polymers, metals or ceramics, which can combat conditions like cancer [9] and fight human pathogens like bacteria [10–14].

For a long time silver has been known to have a disinfecting effect and has found applications in traditional medicines and culinary items. Several salts of silver and their derivatives are commercially employed as antimicrobial agents [15]. Thus, nanoparticles of silver have aptly been investigated for their antibacterial property [11–14]. Commendable efforts have been made to explore this property using electron microscopy, which has revealed size-dependent interaction of silver nanoparticles with bacteria [13]. Nanoparticles of silver have thus been studied as a medium for antibiotic delivery [16], and to synthesize composites for use as disinfecting filters [17] and coating materials [18]. However, the bactericidal property of these nanoparticles depends on their stability in the growth medium, since this imparts greater retention time for bacterium–nanoparticle interaction. There

[5] Both of these authors have contributed equally.
[6] Author to whom any correspondence should be addressed.

 

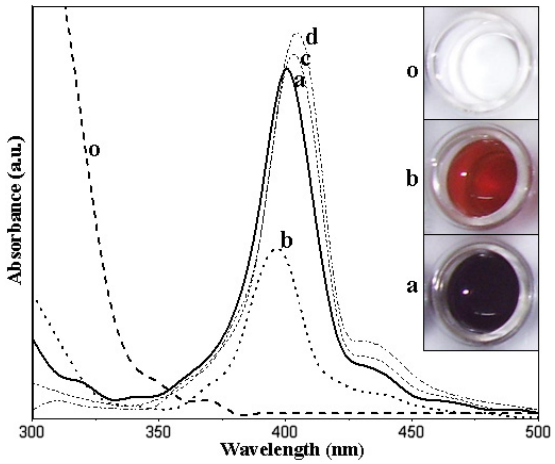


**Figure 1.** UV–visible absorption spectra during various stages of reduction of silver ions to silver nanoparticles and after different ageing times. The inset pictures show the colour changes before (o), during (b) and after the process of reduction (a). The spectra maintain the pattern even after 15 days (c) and a month (d) of preservation under ambient conditions.

lies a strong challenge in preparing nanoparticles of silver stable enough to significantly restrict bacterial growth.

In the present investigation we report the synthesis of highly stable nanoparticles of silver endowed with significant antibacterial properties. Studies were carried out on both antibiotic resistant and non-resistant strains of gram-negative and a non-resistant strain of gram-positive bacteria. A multi-drug resistant strain of gram-negative bacteria was also subjected to analysis to examine the antibacterial effect of the nanoparticles. Efforts have been made to understand the underlying molecular mechanism of such antimicrobial actions. The effect of the nanoparticles was found to be significantly more pronounced on the gram-negative strains, irrespective of whether the strains are resistant or not, than on the gram-positive organisms. We observed a similar extent of antibacterial effect at silver concentrations that are five times less than the previously reported cases [11]. We attribute this enhanced antibacterial effect of the nanoparticles to their stability in the medium as a colloid, which modulates the phosphotyrosine profile of the bacterial proteins and arrests bacterial growth.

## 2. Experimental details

### *2.1. Materials*

Four bacterial strains, namely *Escherichia coli* (ATCC 25922), *Staphylococcus aureus* (ATCC 25923), ampicillin-

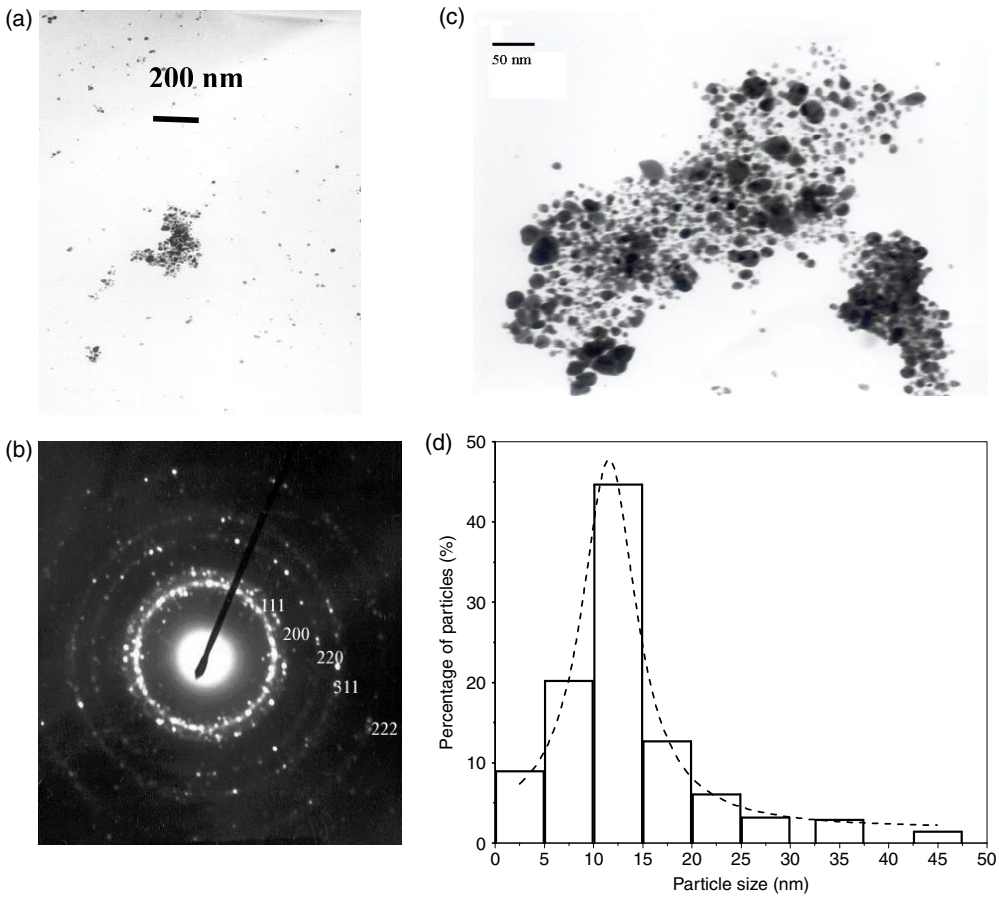


**Figure 2.** TEM micrographs showing spherical silver nanoparticles, and the SAED pattern. (a) Both mono-dispersed and agglomerated nanoparticles of silver; (b) the diffraction pattern of the nanoparticles; (c) higher magnification of the cluster reveals spherical nanoparticles of silver; (d) particle size distribution showing most of the particles in the size range of 10–15 nm.

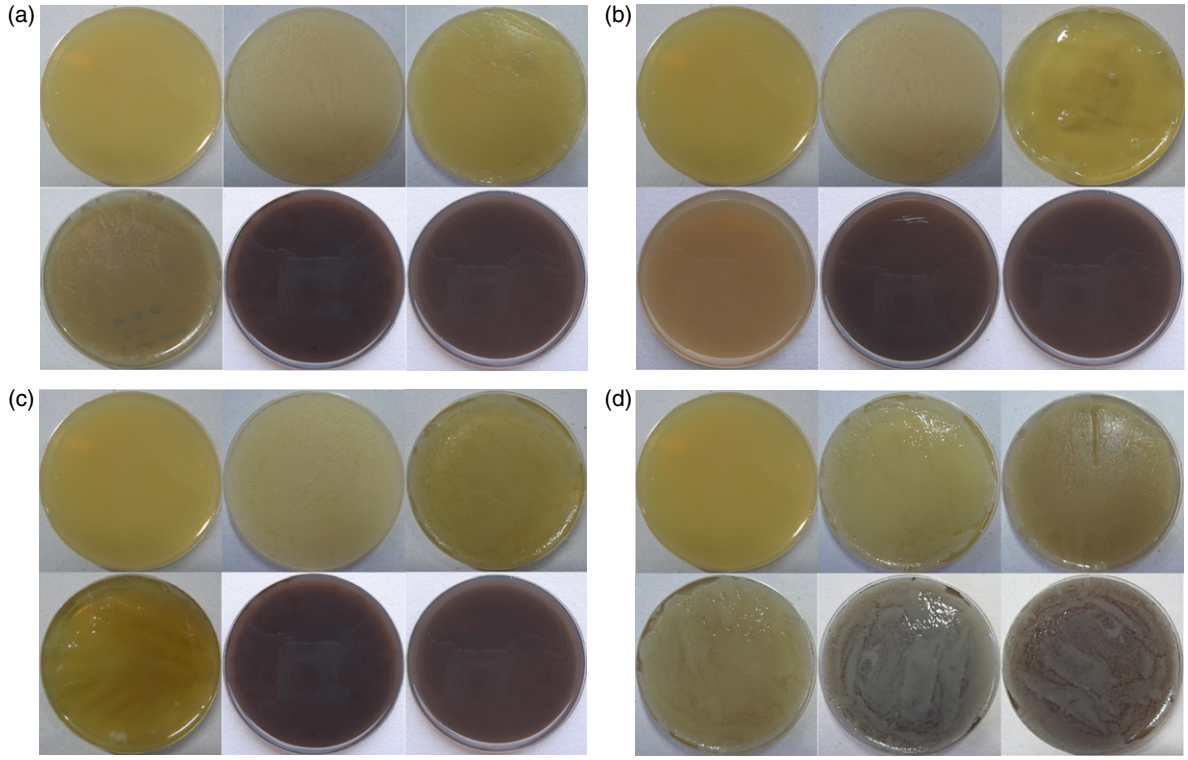


**Figure 3.** Bacteria grown on agar plates at different concentrations of silver nanoparticles. (a) *E. coli*; (b) ampicillin-resistant *E. coli*; (c) multi-drug resistant *S. typhi*; (d) *S. aureus*. In each figure the concentrations of silver nanoparticles are as follows: upper middle, 0 $\mu$g ml$^{-1}$; upper right, 5 $\mu$g ml$^{-1}$; bottom left, 10 $\mu$g ml$^{-1}$; bottom middle, 25 $\mu$g ml$^{-1}$; bottom right, 35 $\mu$g ml$^{-1}$. Upper left plate, agar without nanoparticles and without bacterial inoculation.

resistant *Escherichia coli*, and a multi-drug resistant strain of *Salmonella typhus*, resistant to chloramphenicol, amoxycilin and trimethoprim, were subjected to this analysis. The components of the Luria–Bertani (LB) medium and different antibiotics used in the study were supplied by HiMedia Laboratories, India. Mouse monoclonal antibody against phosphotyrosine (clone 4G10) and horseradish-peroxidase-labelled anti-mouse secondary antibody were procured from Upstate Biotechnology, USA, and Bangalore Genei, India, respectively. The BCA protein assay kit was from Novagen, USA, PVDF membranes were from Bio-Rad, USA, and the enhanced chemiluminescence kit was from Pierce, USA. Analytical grade reagents from Merck India Ltd. and Qualigens Fine Chemicals, India, were used for the synthesis of silver nanoparticles. Milli-Q grade deionized water (Millipore) was used for preparation of the solutions.

### 2.2. Synthesis of silver nanoparticles

A solution of 0.01 M Ag ions was prepared by dissolving 0.017 g $AgNO_3$ in 100 ml of deionized water. During the process additives like ammonia (30%) were added dropwise, so that silver ions formed a stable soluble complex. The solution obtained was used as the precursor for the silver nanoparticles. A blend of reducing agents like D-glucose and hydrazine was used during the synthesis of the nanoparticles. Blending was essential to control the rate of reduction such that an optimum rate was achieved. A higher reducing rate had been shown to form clusters of silver nanoparticles with reduced stability [11]. About 110 ml of such a blend of reducing agents (at a concentration of 0.01 M) was incorporated into 100 ml of silver nitrate stock solution (0.01 M) with continuous stirring. This ensured complete reduction of the silver ions to form silver nanoparticles at a concentration of 0.005 M in aqueous media. The pH of the nanoparticles thus formed was maintained at 7.4 with citric acid (1 M). The brown solutions of Ag nanoparticles were stored in closed glass vials under ambient conditions for future experiments.

### 2.3. Characterization of silver nanoparticles

To verify reduction of silver ions the solution was scanned in the range of 200–600 nm in a spectrophotometer (Pharmacia Biotech) using a quartz cuvette with water as the reference. The size and morphology of the nanoparticles were analysed with a transmission electron microscope (JEOL 200C×). The sample was prepared by placing a drop of silver nanoparticles on carbon-coated copper grid and subsequently drying in air, before transferring it to the microscope operated at an accelerated voltage of 120 kV. The stability of nanoparticles was examined by exposing them to ambient conditions for four weeks, followed by centrifugation (Plasto Crafts) at 15 000*g* for 15 min at RT to rule out formation of precipitate with time. The colour and pH of the solution were also checked at regular intervals, which hardly showed any change.

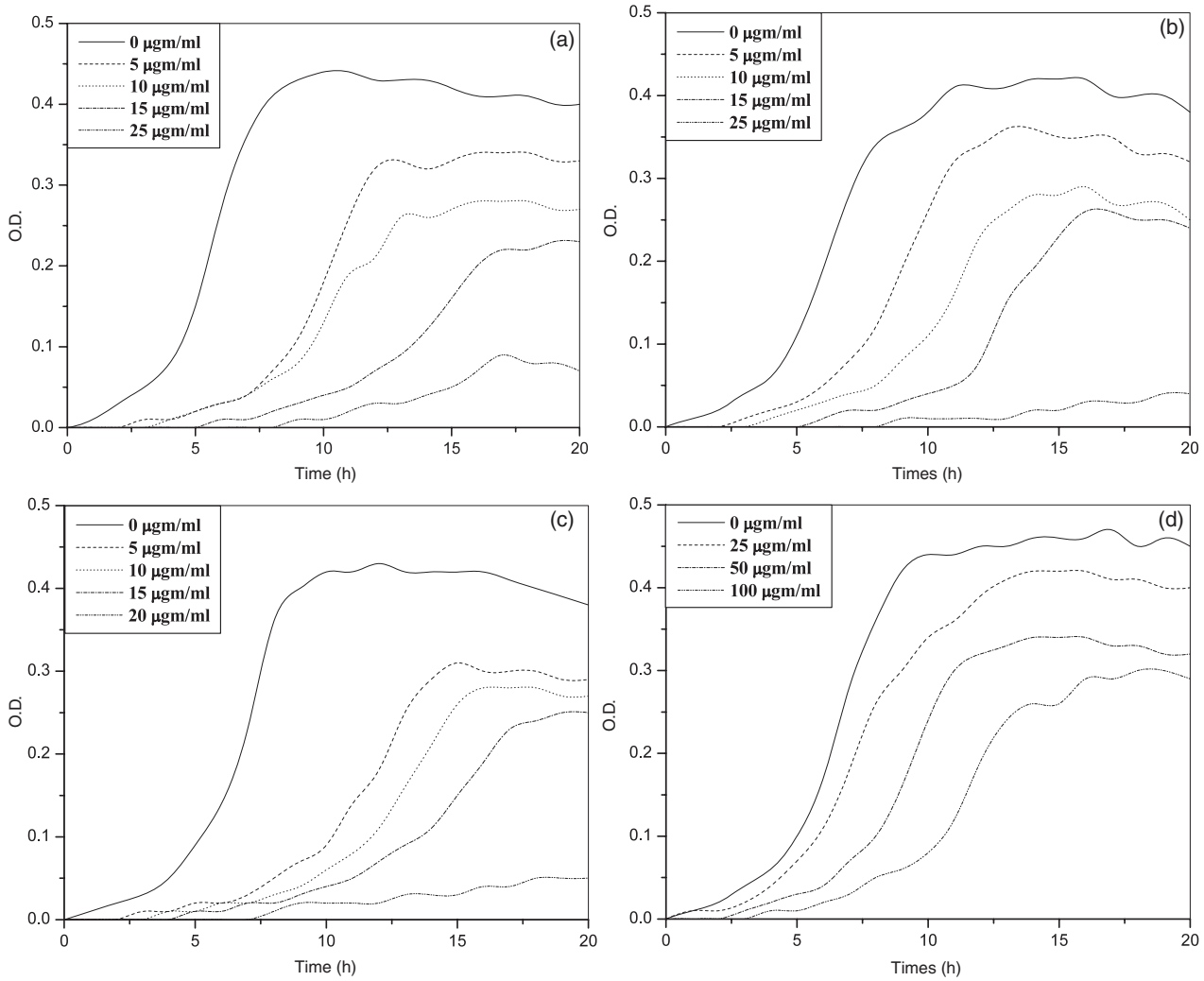


**Figure 4.** Bacterial dynamic growth curve in LB media at different concentrations of silver nanoparticles. (a) *E. coli*; (b) ampicillin-resistant *E. coli*; (c) multi-drug resistant *S. typhi*; (d) *S. aureus*.

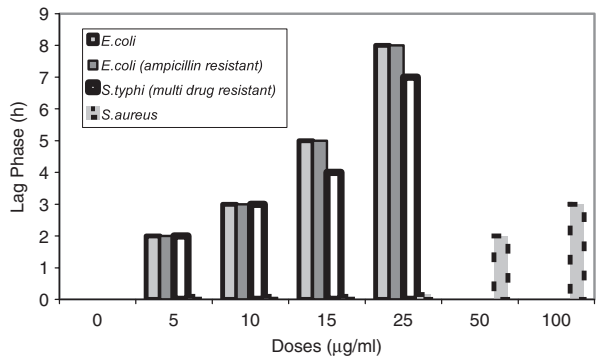


**Figure 5.** Lag phase in the bacterial growth curve at different concentrations of silver nanoparticles.

### *2.4. Analysis of the antibacterial activity of silver nanoparticles*

The effect of silver nanoparticles on gram-negative and gram-positive bacteria was investigated by culturing the organisms on LB agar plates ($10^6$ colony forming units (CFU) of each strain per plate) supplemented with nanoparticles at concentrations of 5, 10, 25 or 35 $\mu$g ml$^{-1}$. Plates without silver nanoparticles were used as controls. Plates were incubated for 24 h at 37 °C and the number of colonies was counted. The counts on three plates corresponding to a particular sample were averaged.

To study growth of bacteria in liquid broth, inoculations were given from fresh colonies on agar plates into 100 ml LB culture medium. Growth was allowed till the optical density reached 0.1 at 600 nm (OD of 0.1 corresponds to a concentration of $10^8$ CFU ml$^{-1}$ of medium). Subsequently, $2 \times 10^8$ CFU from above were added to 100 ml liquid LB media supplemented with 5, 10, 15 or 25 $\mu$g ml$^{-1}$ of silver nanoparticles. Control broths were used without nanoparticles. Antibiotics (ampicillin, 100 $\mu$g ml$^{-1}$; kanamycin, 25 $\mu$g ml$^{-1}$; chloramphenicol, 32 $\mu$g ml$^{-1}$; trimethoprim, 16 $\mu$g ml$^{-1}$; amoxycilin, 40 $\mu$g ml$^{-1}$) were added to different media as appropriate. Growth rate was determined by measuring optical density at 600 nm at regular intervals. In order to further define the effect of silver nanoparticles on gram-positive bacteria, *S. aureus* was exposed to higher doses of silver nanoparticles (50 and 100 $\mu$g ml$^{-1}$) and the growth was studied.

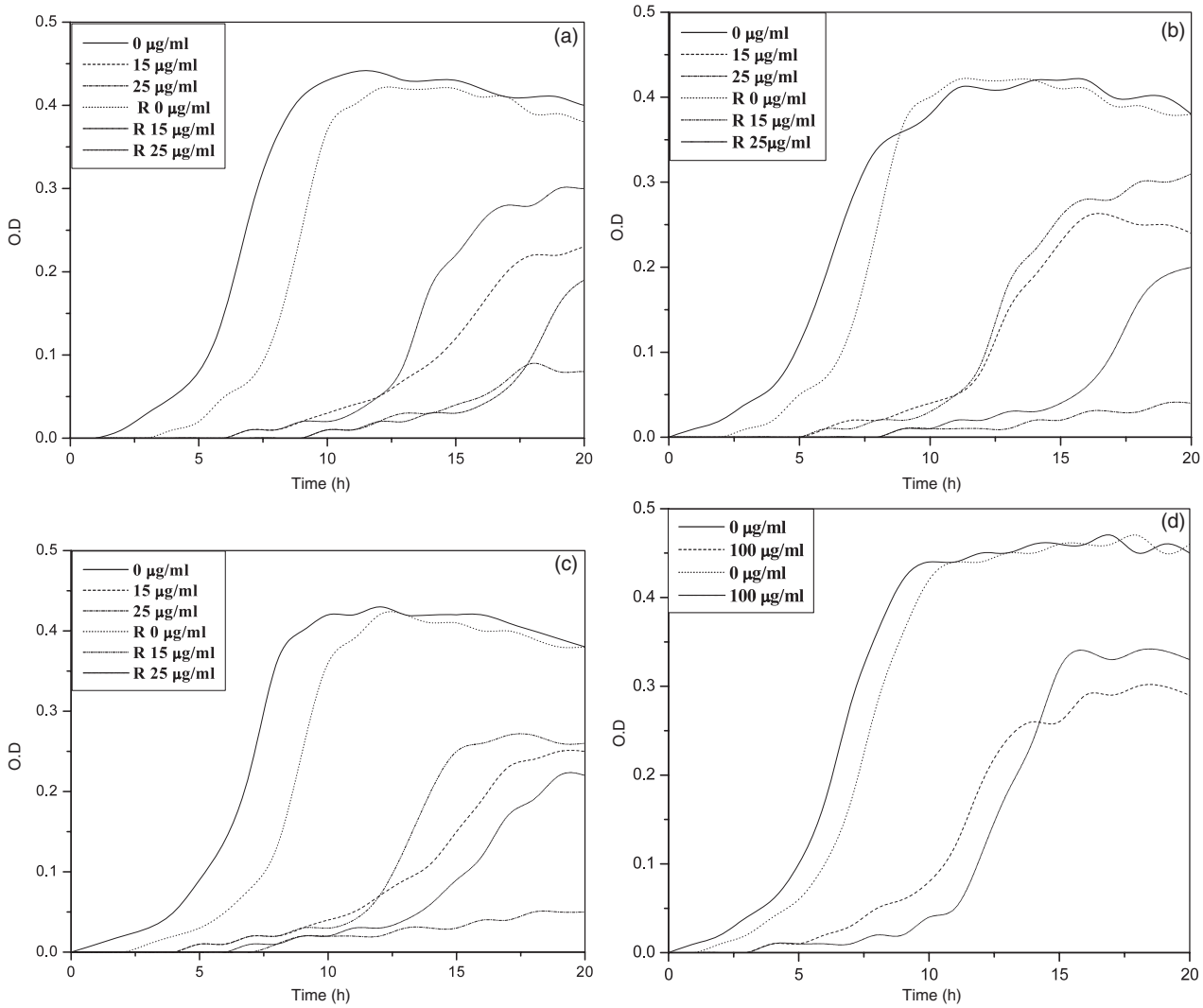


**Figure 6.** Bacterial dynamic growth curve in LB media after sedimentation and resuspension of the bacteria. (a) *E. coli*; (b) ampicillin-resistant *E. coli*; (c) multi-drug resistant *S. typhi*; (d) *S. aureus*.

In other experiments, interaction between bacteria and silver nanoparticles was studied by culturing the cells in LB medium for 60 min in the presence of nanoparticles, then sedimenting the bacteria and reculturing them in fresh medium (without nanoparticles).

### *2.5. Analysis of the phosphotyrosine profile of bacterial proteins*

To study the effect of silver nanoparticles on bacterial signal transduction, strains of bacteria were separately cultured in 100 ml LB media, supplemented without or with varying concentrations of silver nanoparticles, till the OD (at 600 nm) reached 0.1. Cells were collected by centrifugation at 5000*g* for 5 min at 4 °C and were resuspended in 10 ml chilled PBS supplemented with sodium orthovanadate (3 mM). Following 15 min incubation in ice, cells were lysed by sonication (50 W for 10 s, total seven cycles), and centrifuged at 10 000*g* for 5 min at 4 °C. Supernatant was boiled with Laemmli lysis buffer and stored at −20 °C.

Approximately 60 ng bacterial proteins were run on 10–18% gradient polyacrylamide–SDS gels and electroblotted onto PVDF membrane. After blocking with 5% BSA, membranes were incubated for 2 h with monoclonal antibody against phosphotyrosine (clone 4G10) (1:100 dilution),

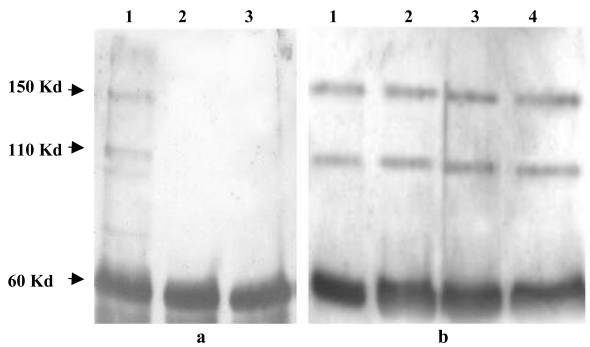


**Figure 7.** Profile of tyrosine phosphorylated proteins obtained from *E. coli* (a) and *S. aureus* (b). In different lanes concentrations of silver nanoparticles are as follows: lane 2, 10 $\mu$g ml$^{-1}$; lane 3, 25 $\mu$g ml$^{-1}$; lane 4, 50 $\mu$g ml$^{-1}$. Lane 1 is without nanoparticles.

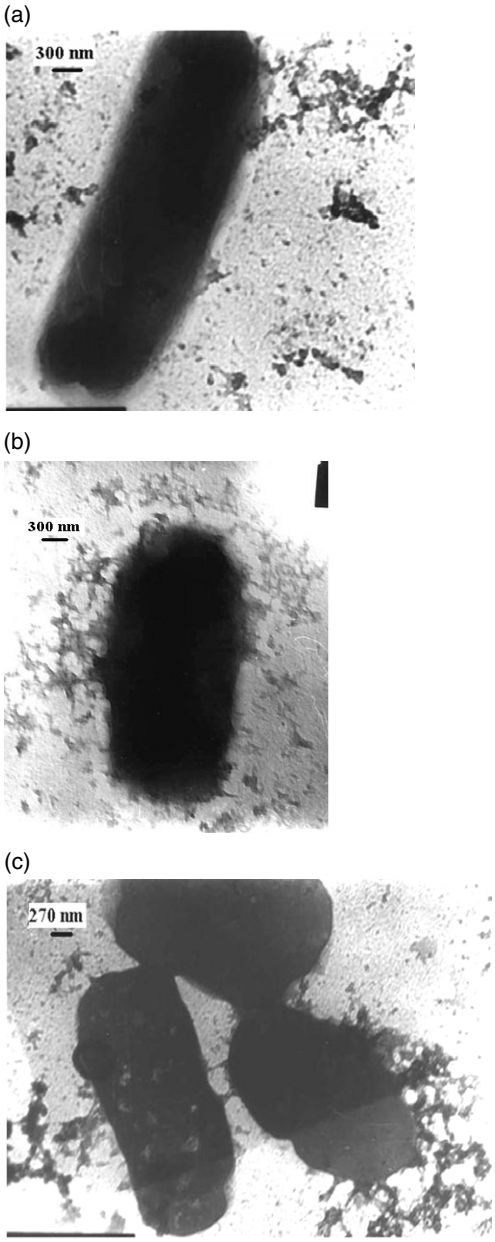


**Figure 8.** TEM microphotographs showing different stages of interaction of silver nanoparticles with *E.coli*.

followed by 1 h incubation with peroxidase-conjugated anti-mouse IgG (dilution 1:5000). The signals were visualized using enhanced chemiluminescence.

## 3. Results and discussion

### *3.1. Reduction kinetics and morphology of silver nanoparticles*

The reduction of silver ions was visibly evident from the colour changes associated with it. Figure 1 shows UV–visible absorption spectra during various stages of reduction of the precursors as they transformed into the silver nanoparticles and after different ageing times during its preservation under ambient conditions. The inset pictures show the colour changes before (o), during (b) and after the process of reduction (a). The silver nitrate solution showed a high at about 300 nm, which gradually underwent red shift with appearance of a hump at 400 nm consistent with formation of silver nanoparticles. The sharp peak at 400 nm can be attributed to a narrow size distribution of the particles formed in the solution. As evident in figure 1 the particles showed hardly any change in the absorption spectra even after a month of ageing time, consistent with the highly stable nature of the nanoparticles. The rate of reaction was optimized to yield partially mono-dispersed silver nanoparticles of uniform size and shape, as shown in the electron micrograph in figure 2(a). The selected area electron diffraction (SAED) pattern obtained from the nanoparticles represented silver having face centred cubic (*fcc*) crystallographic structure. The different diffracting planes were indexed as shown in figure 2(b). Figure 2(c) shows a cluster of silver nanoparticles at higher magnification. The particles were found to be spherical or polyhedral in shape, having a mean size about 10–15 nm. This polyhedral shape could be attributed to the controlled reaction rate, resulting in initial nucleus formation and subsequent growth. Figure 2(d) represents the size distribution plot, suggesting that most of the particles conformed to the size range of 10–15 nm.

### *3.2. Effect of silver nanoparticles on bacterial growth*

LB agar plates incorporating increasing concentrations of silver nanoparticles were inoculated with $10^6$ CFU from different bacterial strains. In case of non-resistant *E. coli* 60% inhibition in bacterial growth was observed in plates supplemented with 5 $\mu$g ml$^{-1}$ of nanoparticles. The extent of inhibition increased to 90% in plates with 10 $\mu$g ml$^{-1}$ nanoparticles, whereas the concentration of 25 $\mu$g ml$^{-1}$ ensured complete inhibition of bacterial growth (figure 3(a)). In the case of ampicillin-resistant *E. coli* and multi-drug resistant strains of *S. typhi*, 70–75% inhibition in growth was observed in plates supplemented with 10 $\mu$g ml$^{-1}$ of nanoparticles, whereas 25 $\mu$g ml$^{-1}$ or higher concentration of nanoparticles elicited 100% inhibition in growth of bacteria (figures 3(b) and (c)). Interestingly, none of the doses of silver nanoparticles had hardly any effect on the growth of *S. aureus* (gram-positive) (figure 3(d)).

In further experiments, strains of gram-negative and gram-positive bacteria were inoculated in liquid LB media supplemented with silver nanoparticles. Increasing concentration of nanoparticles progressively inhibited the growth of non-resistant *E. coli* (figure 4(a)). The lag phase was found to be more prolonged than that described in the earlier reports [11]. This could be attributable to greater stability of the nanoparticles used in this study. The concentration of 25 $\mu$g ml$^{-1}$ was found to be strongly inhibitory for bacteria, as it took about 8 h to initiate any noticeable growth. Similar results were obtained with either resistant or non-resistant strains of other gram-negative bacteria studied (figures 4(b) and (c)).

In contrast, silver nanoparticles were found to have a less significant effect on the growth of gram-positive bacteria (*S. aureus*). No reduction in bacterial growth was observed till the concentration of nanoparticles rose to 25 $\mu$g ml$^{-1}$, whereas the concentration of 100 $\mu$g ml$^{-1}$ elicited only a

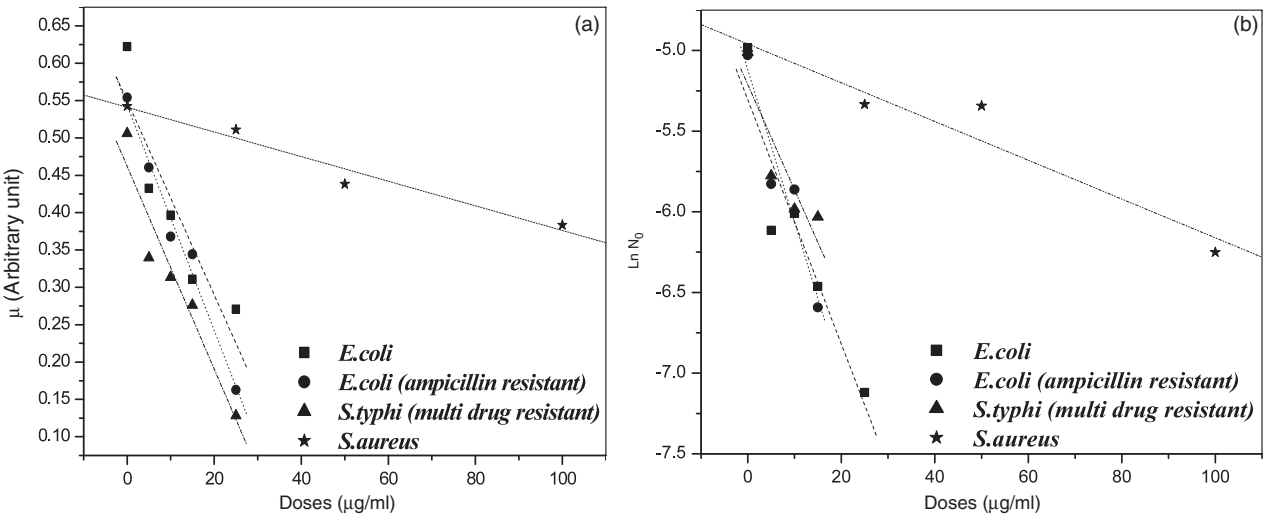


**Figure 9.** Effect of silver nanoparticles on bacterial growth rate constant ($\mu$) (a) and the initial cell count ($L_0$) (b).

partial growth inhibition (figure 4(d)). A shorter lag phase was associated with the growth of gram-positive bacteria treated with nanoparticles, which contrasted with that in the case of the gram-negative strains (figure 5).

Next we explored whether the anti-bacterial effect of the nanoparticles was attributable to the mere presence of these particles in the growth medium, or was the outcome of their interaction with bacterial cellular components. Cells were cultured for 60 min in the presence of silver nanoparticles, followed by sedimentation and re-culturing them in fresh medium without nanoparticles. Control cells were treated similarly but without exposure to the nanoparticles. A significant retardation in growth of re-cultured gram-negative bacteria, and not of gram-positive bacteria, was observed in the fresh medium when they had been originally exposed to the nanoparticles (figure 6). Control cells displayed normal growth characteristics. These observations were consistent with sustained interaction between nanoparticles and cellular components of gram-negative bacteria, as otherwise the growth curves of re-cultured bacteria would have been comparable to that of the control cells.

### *3.3. Effect of silver nanoparticles on the phosphotyrosine profile of bacterial proteins*

In order to study the possible effect of nanoparticles on bacterial signal transduction affecting growth, we examined the phosphotyrosine content of proteins derived from gram-positive and negative bacteria using a specific monoclonal antibody. Phosphorylation of various protein substrates is now well established in bacterial species [19] and is found to influence bacterial signal transduction [20]. Hardly any change in the profile of tyrosine phosphorylated proteins was observed for *S. aureus* upon treatment with silver nanoparticles (figure 7(a)). However, there was noticeable dephosphorylation of two peptides of relative masses 150 and 110 kDa in *E. coli* (figure 7(b)) and *S. typhi* (not shown) exposed to nanoparticles. As tyrosine phosphorylation in bacteria would lead to activation of various protein substrates like RNA polymerase sigma factors and UDP-glucose dehydrogenases [21], decreased phosphorylation may reflect inhibition of activity of these enzymes with critical implications on bacterial growth. A recent report has described tyrosine phosphorylation of bacterial single-stranded DNA-binding proteins (BsSSB), ubiquitous molecules binding DNA in various functional stages like replication and recombination [22]. A phospho-signalling pathway has also been shown to be critical for bacterial cell cycle progression [23]. The identity of the substrate peptides and that of the putative tyrosine phosphatases responsible for observed dephosphorylation in gram-negative bacteria, as described in this report, are yet to be established and can be the subject for future research. The present findings, along with reported interactions of silver nanoparticles with thiol-rich enzymes and bacterial genomic DNA [13], can explain the inhibitory effect of the nanoparticles on growth of gram-negative bacteria. Interestingly, phosphorylation of protein tyrosine kinases involved in exopolysaccharide and capsular polysaccharide biosynthesis and transport has been reported in a number of gram-negative and gram-positive bacteria [24].

### *3.4. Transmission electron microscopy*

Different stages of interaction between gram-negative bacteria and silver nanoparticles are illustrated in the transmission electron microphotographs (figure 8). In the initial stages of interaction, clusters of nanoparticles were found to anchor to the bacterial cell wall (figure 8(a)), possibly at sites that are rich in negatively charged functional groups. Later, the nanoparticles manage to enter the bacterial cell (figure 8(b)). In another micrograph (figure 8(c)) the nanoparticles were observed to anchor the cell at several sites and make perforations in the membrane, which could result in cell lysis. The interaction of the nanoparticles was found to be much less with the gram-positive organisms (not shown). During later stages of experiment black debris was observed to be precipitated. This might be composed of contents of the cell and nanoparticles and possibly represent a defence mechanism to locally deplete silver concentration. The cumulative effect

of these factors would lead to retardation in bacterial growth but not complete annihilation.

### *3.5. Prediction of bacterial growth in the presence of varying concentrations of silver nanoparticles*

The dynamic growth rate of a bacterial species is represented by the equation

$$\ln N = \ln L_0 + \mu t \tag{1}$$

where $N$ is the bacterial cell count at time $t$, $L_0$ is the initial cell count and $\mu$ is the growth rate constant for the bacteria. The experimental data were plotted in the logarithmic scale to derive the values of $\mu$ and $\ln L_0$ corresponding to various doses of the nanoparticles ($x$) studied. Linear relationships between $x$ and $\mu$ (figure 9(a)) and $x$ and $L_0$ (figure 9(b)) were derived for each of the species of bacteria investigated as shown below:

$$\mu = -ax + b \tag{2}$$

$$\ln L_0 = -cx - d \tag{3}$$

where $a$, $b$, $c$ and $d$ are the constants for the respective bacteria as below.

| Name of the bacterium | $a$ | $b$ | $c$ | $d$ |
|---|---|---|---|---|
| *E. coli* | 0.0649 | 0.5494 | 0.3783 | 5.3061 |
| *E. coli* (ampicillin resistant) | 0.0753 | 0.5435 | 0.4727 | 5.1190 |
| *S. typhi* (multi-drug resistant) | 0.0678 | 0.4618 | 0.3263 | 5.2115 |
| *S. aureus* | 0.0082 | 0.541 | 0.0601 | 4.9598 |

Similar relationships, though in complex forms, have been proposed for several chemical species affecting the bacterial growth [25].

Thus, by replacing the values of $\mu$ and $\ln L_0$, equation (1) can be rewritten as

$$\ln N = (bt - d) - (at + c)x. \tag{4}$$

Equation (4) represents the dynamic growth rate of bacteria in the presence of different concentrations of silver nanoparticles in the medium. It can be noticed that slopes of the trend lines representing gram-positive bacteria are an order of magnitude less than those for the gram-negative strains (figures 9(a) and (b)), which is consistent with the observed impairment of growth in the case of gram-negative bacteria in the presence of silver nanoparticles.

### *3.6. Possible mechanism for antibacterial action of silver nanoparticles*

The differences between gram-positive and gram-negative bacteria essentially rest in the structure of their respective cell walls. The gram-negative bacteria have a layer of lipopolysaccharide at the exterior, followed underneath by a thin (about 7–8 nm) layer of peptidoglycan [26]. Although the lipopolysaccharides are composed of covalently linked lipids and polysaccharides, they lack strength and rigidity. Negative charges on the lipopolysaccharides [28] are attracted towards weak positive charges available on silver nanoparticles [29]. On the other hand, the cell wall in gram-positive bacteria is principally composed of a thick layer (about 20–80 nm) of peptidoglycan, consisting of linear polysaccharide chains cross-linked by short peptides to form a three dimensional rigid structure [27]. The rigidity and extended cross-linking not only endow the cell walls with fewer anchoring sites for the silver nanoparticles but also make them difficult to penetrate. The extent of inhibition of bacterial growth reported in this study was dependent on the concentration of nanoparticles in the medium. Interaction between nanoparticles and the cell wall of bacteria would be facilitated by the relative abundance of negative charges on the gram-negative bacteria, which was congenial to the fact that growth of gram-negative bacteria was more profoundly affected by the silver nanoparticles than that of the gram-positive organisms. As demonstrated by electron microscopy, interaction with nanoparticles resulted in perforations in the cell wall, contributing to the antibacterial effects of the nanoparticles. Inferences from the reculture experiments were consistent with the entry of nanoparticles inside bacterial cells and/or strong association with bacterial cellular components. Once inside the cell, nanoparticles would interfere with the bacterial growth signalling pathway by modulating tyrosine phosphorylation of putative peptide substrates critical for cell viability and division.

## 4. Conclusion

The silver nanoparticles synthesized and analysed in this report were found to have stronger antibacterial potency than those described in the earlier reports [11, 13]. The effect was dose dependent and was more pronounced against gram-negative organisms than gram-positive ones. The antibacterial effect of nanoparticles was independent of acquisition of resistance by the bacteria against antibiotics. The major mechanism through which silver nanoparticles manifested antibacterial properties was by anchoring to and penetrating the bacterial cell wall, and modulating cellular signalling by dephosphorylating putative key peptide substrates on tyrosine residues. However, further studies must be conducted to verify if the bacteria develop resistance towards the nanoparticles and to examine cytotoxicity [30] of nanoparticles towards human cells before proposing their therapeutic use.

## Acknowledgments

This research was funded by the Indian Council of Medical Research (ICMR) and the DST Unit on Nanoscience and Technology (DST-UNANST), BHU. We sincerely thank Dr G K Dey of the Bhaba Atomic Research Center, Mumbai, for carrying out the TEM analysis of the nanoparticles and Professor O N Srivastava for encouragement. TB acknowledges Professor S Lele and Dr R K Mandal of BHU for valuable discussions and encouragement.

## References

[1] Gleiter H 2000 Nanostructured materials, basic concepts and microstructure *Acta Mater.* **48** 1–12
[2] Curtis A and Wilkinson C 2001 Nanotechniques and approaches in biotechnology *Trends Biotechnol.* **19** 97–101

[3] Waren C W and Nie S 1998 Quantum dot bioconjugates for ultra sensitive nonisotopic detection *Science* **281** 2016–8

[4] Vaseashta A and Dimova-Malinovska D 2005 Nanostructured and nanoscale devices, sensors and detectors *Sci. Technol. Adv. Mater.* **6** 312–8

[5] Langer R 2001 Drug delivery: drugs on target *Science* **293** 58–9

[6] Roy K, Mao H Q, Huang S K and Leong K W 1999 Oral gene delivery with Chitosan-DNA nanoparticles generates immunologic protection in a murine model of peanut allergy *Nat. Med.* **5** 387–91

[7] Sachlos E, Gotora D and Czernuszka J T 2006 Collagen scaffolds reinforced with biomimetic composite nano-sized carbonate-substituted hydroxyapatite crystals and shaped by rapid prototyping to contain internal microchannels *Tissue Eng.* **12** 2479–87

[8] Xu Z P, Zeng Q H, Lu G Q and Yu A B 2006 Inorganic nanoparticles as carriers for efficient cellular delivery *Chem. Eng. Sci.* **61** 1027–40

[9] Farokhzad O C, Cheng J, Teply B A, Sherifi I, Jon S, Kantoff P W, Richie J P and Langer R 2006 Targeted nanoparticle-aptamer bioconjugates for cancer chemotherapy *in vivo Proc. Natl Acad. Sci. USA* **103** 6315–20

[10] Stoimenov P K, Klinger R L, Marchin G L and Klabunde K J 2002 Metal oxide nanoparticles as bactericidal agents *Langmuir* **18** 6679–86

[11] Sondi I and Salopek-Sondi B 2004 Silver nanoparticles as antimicrobial agent: a case study of *E. coli* as a model for gram-negative bacteria *J. Colloids Interface Sci.* **275** 177–82

[12] Panacek A, Kvitek L, Prucek R, Kolar M, Vecerova R, Pizurova N, Sharma V K, Nevecna T and Zboril R 2006 Silver colloid nanoparticles: synthesis, characterization, and their antibacterial activity *J. Phys. Chem.* B **110** 16248–53

[13] Morones J R, Elechiguerra J L, Camacho A, Holt K, Kouri J B, Ramirez J T and Yacaman M J 2005 The bactericidal effect of silver nanoparticles *Nanotechnology* **16** 2346–53

[14] Baker C, Pradhan A, Pakstis L, Pochan D J and Shah S I 2005 Synthesis and antibacterial properties of silver nanoparticles *J. Nanosci. Technol.* **5** 244–9

[15] Holladay R, Moeller W, Mehta D, Brooks J, Roy R and Mortenson M 2006 Silver/water, silver gels and silver-based compositions; and methods for making and using the same *Application Number* WO2005US47699 20051230 European Patent Office

[16] Li P, Li J, Wu C, Wu Q and Li J 2005 Synergistic antibacterial effects of $\beta$-lactam antibiotic combined with silver nanoparticles *Nanotechnology* **16** 1912–7

[17] Jain P and Pradeep T 2005 Potential of silver nanoparticle-coated polyurethane foam as an antibacterial water filter *Biotechnol. Bioeng.* **90** 59–63

[18] Li Y, Leung P, Yao L, Song Q W and Newton E 2006 Antimicrobial effect of surgical masks coated with nanoparticles *J. Hosp. Infec.* **62** 58–63

[19] Deutscher J and Saier M H 2005 Ser/Thr/Tyr protein phosphorylation in bacteria—for long time neglected, now well established *J. Mol. Microbiol. Biotechnol.* **9** 125–31

[20] Kirstein J and Turgay K 2005 A new tyrosine phosphorylation mechanism involved in signal transduction in *Bacillus subtilis J. Mol. Microbiol. Biotechnol.* **9** 182–8

[21] Mijakovic I, Petranovic D, Bottini N, Deutscher J and Ruhdal Jensen P 2005 Protein tyrosine phosphorylation in *Bacillus subtilis J. Mol. Microbiol. Biotechnol.* **9** 189–97

[22] Mijakovic I, Petranovic D, Macek B, Cepo T, Mann M, Davies J, Jensen P R and Vujaklija D 2006 Bacterial single-stranded DNA—binding proteins are phosphorylated on tyrosine *Nucleic Acids Res.* **34** 1588–96

[23] Iniesta A A, McGrath P T, Reisenauer A, McAdams H H and Shapiro L 2006 A phosphor signaling pathway controls the localization and activity of a complex critical for bacterial cell cycle progression *Proc. Natl Acad. Sci. USA* **103** 10935–40

[24] Grangeasse C, Obadia B, Mijakovic I, Deutscher J, Cozzone A J and Doublet P 2003 Autophosphorylation of the *Escherichia coli* kinase Wzc regulates tyrosine phosphorylation of Ugd, a UDP-glucose dehydrogenase *J. Biol. Chem.* **278** 39323–39

[25] Nostro P L, Ninham B W, Nostro A L, Pesavento G, Fratoni L and Baglioni P 2005 Specific ion effects on the growth rates of *Staphylococcus aureus* and *Pseudomonas aeruginosa Phys. Biol.* **2** 1–7

[26] Madigan M and Martinko J 2005 *Brock Biology of Microorganisms* 11th edn (Englewood Cliffs, NJ: Prentice Hall)

[27] Baron S 1996 *Medical Microbiology* 4th edn (Galveston: University of Texas Medical Branch)

[28] Salton M R J and Kim K S 1996 Structure *Baron's Medical Microbiology* 4th edn (Galveston: University of Texas Medical Branch)

[29] Sui Z M, Chen X, Wang L Y, Xu L M, Zhuang W C, Chai Y C and Yang C J 2006 Capping effect of CTAB on positively charged Ag nanoparticles *Physica* E **33** 308–14

[30] Braydich-Stolle L, Hussain S, Schlager J J and Hofmann M C 2005 *In vitro* cytotoxicity of nanoparticles in mammalian germline stem cells *Toxicol. Sci.* **88** 412–9